Digital All-Optical Signal Processing Using Microdisc Lasers

J. Hofrichter[1], F. Horst[1], N. Chrysos[1], C. Minkenberg[1], R. Kumar[2], L. Liu[2], G. Morthier[2], T. de Vries[3], and B.J. Offrein[1]

1: IBM Research GmbH, IBM Research – Zurich, Säumerstrasse 4, 8803 Rüschlikon, Switzerland
2: Photonics Research Group, INTEC Department, Ghent University – IMEC, St. Pietersnieuwstraat 41, 9000 Ghent, Belgium
3: COBRA Research Institute, Eindhoven University of Technology, PO. Box 512, 5600MB Eindhoven, The Netherlands

Abstract: Microdisc lasers (MDLs) are becoming a viable option for compact laser sources, wavelength converters and even all-optical memory on a chip. Therefore we have developed a fast and accurate compact model for MDLs suitable for simulating these functionalities. The simulations are compared with measurements of MDLs operated as all-optical flip-flops. Minimum switching energies are extracted and compared with state-of-the art electronics. Furthermore we present the fan-out and signal refreshing properties of MDLs making the device suitable for all-optical logic applications.

OCIS codes: (000.0000) General; (000.0000) General

1. Introduction

Microdisc lasers (MDLs), see Fig. 1, which are heterogeneously integrated on silicon wafers [1], are an interesting candidate for on-chip laser sources [2], all-optical wavelength converters [3] and also all-optical memories [5,6]. They are regarded as a viable candidate for all-optical signal processing and photonic switching applications. Within a MDL, several modes compete. Due to the free spectral range of the cavity and the broad gain spectrum of the MQW gain material, typically three lasing peaks are present. Each peak contains two counter-propagating modes.

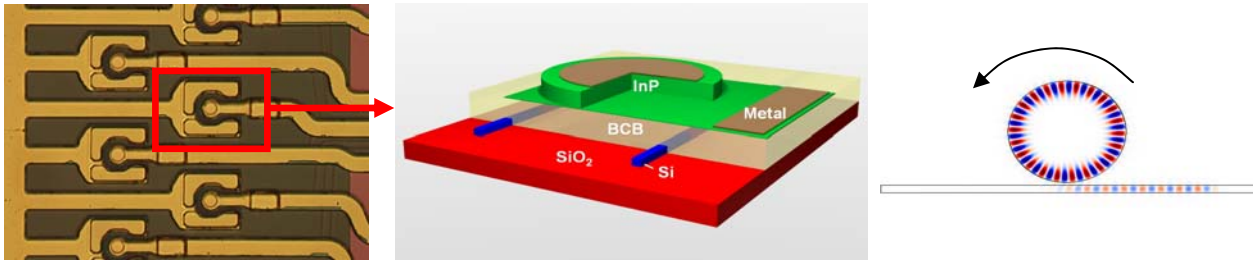

(a) (b) (c)

Fig. 1 – A MDL on a SOI waveguide: (a) microscope image, (b) cross section, (c) field profile with a dominant counter-clockwise (CCW) mode.

2. The 1D microdisc laser model

To accurately simulate the switching behavior of a MDL, we implemented a 1D laser rate equation model. We expanded the model suggested by Van Campenhout *et al.* [1] for self- and cross-gain suppression with the corresponding factors ε_S and ε_C [7-9]. A parabolic gain curve was assumed to account for the nonuniform gain spectrum [10]. Equation (1) gives the radially dependent gain term where G_0 is the maximum gain at the central lasing mode λ_0 and a is the gain curvature parameter. To save computation time and speed up the model, the photon densities $S_{cw,ccw,i}$ are modelled as lumped photon densities of the i-th mode with the corresponding propagation direction. Because we have a quantum well active material for the given devices, logarithmic gain is assumed with the threshold carrier density N_0.

$$g_{CW,CCW}(S_{CW},S_{CCW},n(r),r)=G_0\left[1-a(\lambda_0-\lambda)^2\right]\cdot(1-\varepsilon_S\sum_i S_{CW,CCW,i}-\varepsilon_C\sum_i S_{CCW,CW,i})\cdot\ln\frac{n(r)}{N_0} \quad (1)$$

In Eq. (2), the carrier density $n(r)$ is locally reduced by stimulated emission into the corresponding mode. Therefore the overlap with the modal distribution is being calculated. The modal distribution $\Psi(r)$ is a normalized Bessel function of the first kind $J_\nu(r/z_0)$, where ν is the azimuthal order of the corresponding mode and z_0 being the first Bessel zero of $J_\nu(z)$. The modal distribution is normalized such that $\int_0^R \Psi^2(r)rdr=1$.

$$\frac{\partial n(r)}{\partial t}=-\left[\sum_i g_{CW,i}(r)S_{CW,i}+\sum_i g_{CCW,i}(r)S_{CCW,i}\right]v_g\Psi^2(r)\Gamma\pi R^2-An(r)-Bn(r)^2-Cn(r)^3+\frac{\eta I}{\pi R^2 q t_a}+D\left(\frac{\partial n(r)}{\partial r}+\frac{\partial^2 n(r)}{r\partial r^2}\right) \quad (2)$$

Besides stimulated emission into the respective lasing modes, also nonlasing recombination is taken into account by the coefficients A, B and C for one-, two- and three-particle processes, respectively. The electrical pumping current I flowing through the disk area πR^2 generates charge carriers in the active region, which has thickness t_a. In contrast to

Eqs. (1) and (2) the photon densities defined in Eq. (3) are modelled by lumped variables that obtain their spatial dependence from the modal distribution Ψ(r). Each photon density experiences a decay time constant τ_p due to, e.g., scattering or absorption. The built-up of the mode is achieved by stimulated emission with the modal gain $g_{CW,CCW,i}$ in the active region that has an overlap Γ with the mode. Also, spontaneous emission with the factor B is coupled into the lasing mode with the spontaneous emission coupling factor β. In addition, scattering due to sidewall roughness causes a coupling of the counter-propagating modes, which is modelled by k_{int} [11]. The external injection coupling factor k_{ext} models the coherent external injection [8] of light into the respective lasing mode. Table I lists the values used for the parameters in the model. The model's radial dependency allows for the simulation of spatial hole-burning which limits output power, modal recovery and thus the device speed.

$$\frac{\partial S_{CW,CCW,i}}{\partial t} = -\frac{S_{CW,CCW,i}}{\tau_p} + 2\pi\beta\int_0^R Bn^2(r)\Psi^2(r)r\partial r + S_{CW,CCW,i}\Gamma v_g 2\pi\int_0^R g_{CW,CCW,i}(r)\Psi^2(r)r\partial r \quad (3)$$
$$+k_{\text{int}}S_{CCW,CW,i} + k_{ext}\sqrt{S_{ext,CW,CCW,i}S_{CW,CCW,i}}$$

Table I. Simulation parameters

Param.	R	G_0	N_0	ε_s	ε_c	k_{int}	k_{ext}	v_g	λ_0
Value	3.75 μm	1500cm^{-1}	1.5e18cm^{-3}	2e-17 cm^3	4e-17	1.5e8 s^{-1}	8.8e10s^{-1}	8.817e9 cm s^{-1}	1550 nm
Param.	A	B	C	D	β	η	I	a	t_a
Value	1e-8s^{-1}	2e-10 cm^3 s^{-1}	1.63e-28 cm^6 s^{-1}	8 cm^2 s^{-1}	1e-3	0.267	3.5 mA	1.3e13 cm^{-3}	18 nm

3. Simulations and experiments

To determine the switching speed and energy of the MDLs, experiments and simulations were carried out in which a constant electrical DC current was applied to the device. Optical pulses with an estimated switching energy of 1.8 fJ having a duration of 100 ps and a power of 18 μW were injected into the waveguide in both the experiment and the simulations to investigate the switching behavior of the counter-propagating modes. Details on the experiment can be found in [6]. The curves for the rising edge of the CW mode in the experiment and the simulations are shown in Fig. 3(a). In the experiment, the injection pulse in the waveguide cannot be separated from the MDL output lasing power. However, the simulations provide insight into these modal dynamics and reveal a slight overshoot of the lasing mode. Also the emitted power level can be related to the injection power level in the waveguide. With the parameters and bias conditions given in Table 1, the MDL emits 71 μW and can be switched with only 18 μW leading to a fan-out of $F = P_{MDL}/P_{SW} > 3$ demonstrating MDL signal refreshing and fan-out properties, which are crucial for all-optical logic [12]. In Fig. 3(b) the falling edge of the CCW mode is shown, and a switching time of approx. 60 ps is extracted from both the experiment and the simulations. Not only the switching time shows perfect agreement between experiment and simulation, but also the shape of the falling edge. This is attributed to the lateral discretization of the 1D model in which the modal and carrier dynamics can be simulated. Furthermore, the spatial hole burning of the carrier density can be temporally resolved as presented, see Fig. 3(c). The carrier density is only reduced close to the perimeter of the MDL where the mode is located. However, if a pulse is injected and the state is switched, variations in the carrier density can be observed at t_1=50 ps. However, these variations are fairly low and only visible for the time of the overshooting photon densities in Figs. 3(a) and (b). This leads to the conclusion that the switching times are limited by the optical injection and suppression of the lasing mode rather than by a relaxation oscillation, in which an exchange of the power between the charge carrier density and the modal intensity takes place, which should have been observable in Fig. 3(c). Instead, switching between the two states is achieved when the external light injection is sufficiently long and with a sufficient energy to support the lasing of the suppressed mode. Thereby the dominant mode is suppressed by the non-linear gain suppression. When the intensity

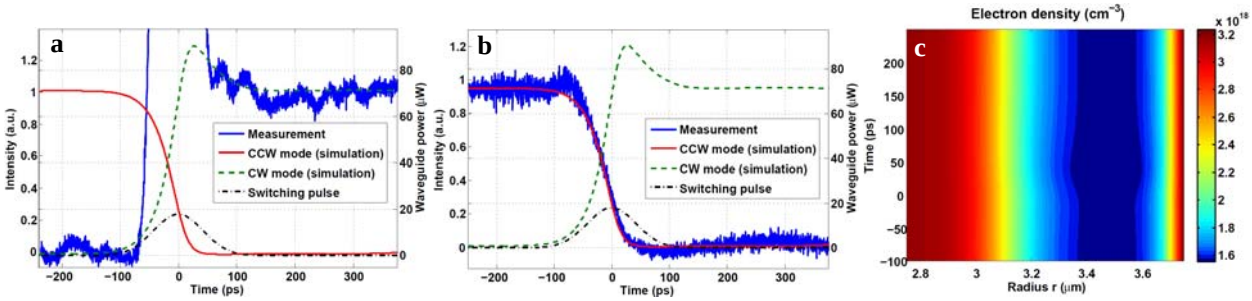

Fig. 3 – Switching properties of a bi-stable MDL: Simulation and measurement of (a) the rising edge and (b) the falling edge. (c) Electron density

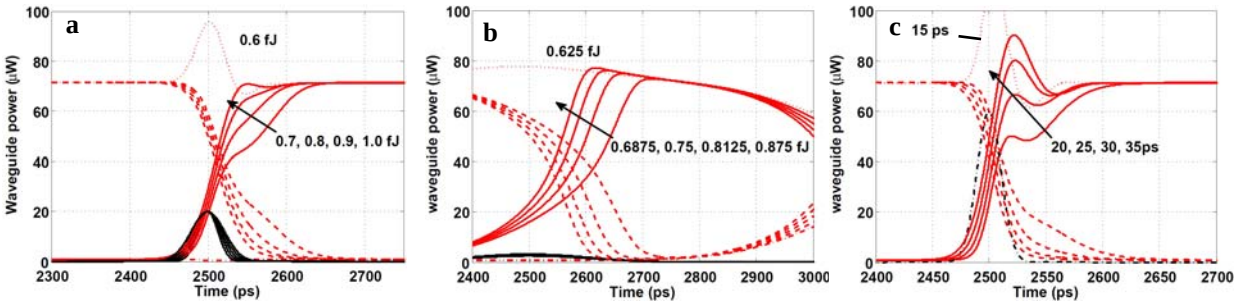

Fig. 4 – Switching properties of a bi-stable MDL: Simulation and measurement of (a) 20 μW, (b) 250 ps, and (c) 60 μW injection.

of the supported mode exceeds that of the dominant mode, the system flips and suppresses the previously dominant mode even further. Now, the other mode is stable suppressing the previously dominant mode until an external injection is applied. Further simulations were performed to investigate minimum switching energies and –times. Under the same bias conditions and with a lowered pulse width a minimum switching energy of 0.7 fJ was. As indicated in Fig. 4(a), shorter pulses did not result in a switching of the state. To investigate the power limit for the switching process, simulations with a fixed pulse length of 250 ps and varying optical power were performed. For 2.5 μW, being equivalent to an energy of 0.625 fJ, no switching could be observed. However, an injection power of 2.75 μW and a corresponding pulse energy of below 0.7 fJ resulted in a switching of the state as shown in Fig. 4(b). To investigate the ultimate switching speed of the device, a relatively high power level of 60 μW was injected into the waveguide. The power level is still lower than the output power of the MDL needed to simulate e.g. a chain of equivalent MDLs in a system. The pulse width has been varied from 15 to 35 ps as presented in Fig. 4(c). While a switching pulse of 15 ps is too short, a pulse width of 20 ps is sufficient to reverse the state of the MDL. The corresponding switching energy of 1.2 fJ is still very small and comparable with that of low-power CMOS circuitry. However, even at these low switching energies, the speed of MDLs by far exceeds that of CMOS electronics [13].

4. Conclusion

We have presented a fast and comprehensive model for the simulation of MDLs. Besides wavelength conversion, also bi-stability can be simulated. The measurements that accompanied the numerical studies showed excellent agreement with the numerical model. Simulations and experiments consistently demonstrate the low-power switching, signal refreshing and fan-out properties of MDLs. The model holds the promise to enable the exploration of further functionalities of MDLs and to guide experimental work in the future.

5. Acknowledgment

The authors acknowledge the financial support by the European Union FP7-ICT project “HISTORIC under contract no. 223876 and inspiring discussions with O. Raz and H.J.S. Dorren, TU Eindhoven, the Netherlands.

[1] J. v. Campenhout, P. Rojo-Remeo, P. Regreny, C. Seassal, D. v. Thourhout, S. Verstuyft, L. Di Cioccio, J.-M. Fedeli, C. Lagahe and R. Baets, “Electrically pumped InP-based microdisk lasers integrated with a nanophotonic silicon-on-insulator waveguide circuit,” Opt. Express **15**(11), 6744–6749 (2007).

[2] L. Liu, J. v. Campenhout, P. Rojo-Romeo, P. Regreny, C. Seassal, D. v. Thourhout, S. Verstuyft, L. Di Cioccio, J.-M. Fedeli, C. Lagahe and R. Baets, “Compact multiwavelength laser source based on cascaded InP-microdisks coupled to one SOI waveguidem” in OSA Technical Digest “Optical Fiber Communication Conf. and Exposition and The National Fiber Optic Engineers Conf.” (OSA, 2008), paper OWQ3.

[3] O. Raz, “High speed wavelength conversion in a heterogeneously integrated disc laser over silicon on insulator for network on a chip applications,” Proc. ECOC, Vienna, Austria, 2009.

[5] M.T. Hill, “A fast low-power optical memory based on coupled micro-ring lasers,” Nature **432**, 206-209 (2004).

[6] L. Liu, R. Kumar, K. Huybrechts, T. Spuesens, G. Roelkens, E.-J. Geluk, T. d. Vries, P. Regreny, D. v. Thourhout, R. Baets and G. Morthier, “An ultra-small, low-power, all-optical flip-flop memory on a silicon chip,” Nature Photonics **268**, 1-6 (2010).

[7] W.E. Lamb, Jr., “Theory of an optical maser,” Phys. Rev. A **134**, 1429-1450 (1964).

[8] C.L. Tang A. Schremer and T. Fujita, “Bistability in two-mode semiconductor lasers via gain saturation,” Appl. Phys. Lett. **51**(18), 1392-1394 (1987).

[9] G. Yuan and S. Yu, “Bistability and switching properties of semiconductor ring lasers with external optical injection,” IEEE J. Quantum Electron.,**44**(1), 41-48, 2008.

[10] M.J. Adams and M. Osihski, “Longitudinal mode competition in semiconductor lasers: Rate equations revisited,” IEE Proc., Part I: Solid State Electron Devices **129**(6), 271-274 (1982).

[11] R. Kumar, L. Liu, G. Roelkens, G. Morthier and R. Baets, “Simple and accurate measurements to characterize microdisk lasers for all-optical flip-flop operation,” Proc. Ann. Symp. IEEE Photonics Benelux Chapt., Belgium (2009).

[12] D.A.B. Miller, “Are optical transistors the logical next step?”, Nature Photonics **4**, 3-5, (2010).

[13] Y. Leblebici, “Leakage current reduction using subthreshold source-coupled logic”, IEEE Trans. Circ. Syst. II, **56**(5), 347-351 (2009).